Spin torque switching in nanopillars with antiferromagnetic reference layer

Arora, M.; Fowley, C.; Mckinnon, T.; Kowalska, E.; Sluka, V.; Deac, A. M.; Heinrich, B.; Girt, E.;

Originally published:

October 2016

IEEE Magnetics Letters 8(2016)1, 3100605

DOI: https://doi.org/10.1109/LMAG.2016.2617319

Spin torque switching in nanopillars with antiferromagnetic reference layer

Monika Arora[1], Ciaran Fowley[2], Tommy McKinnon[1], Ewa Kowalska[2], Volker Sluka[3], Alina Maria Deac[2], Bret Heinrich[1], and Erol Girt[1],
[1]Department of Physics, Simon Fraser University, Burnaby, British Columbia, V5A 1S6, Canada.
[2]Helmholtz-Zentrum Dresden-Rossendorf, Institute of Ion Beam Physics and Materials Research, 01328 Dresden, Germany.
[3]Department of Physics, New York University, New York, NY 10003, USA.

Spin-transfer-torque induced switching is investigated in 200 nm diameter circularly shaped, perpendicular magnetized nanopillars. A synthetic antiferromagnet, consisting of two Co/Ni multilayers coupled anti-ferromagnetically across a Ru layer, is used as a reference layer to minimize the dipolar field on the free layer. The free layer is a single 4×[Co/Ni] multilayer. The use of Pt and Pd was avoided to lower the spin-orbit scattering in magnetic layers and intrinsic damping in the free layer, and therefore, reduce the critical current required for spin-transfer-torque switching. The intrinsic Gilbert damping of a continuous 4×[Co/Ni] multilayer film was measured by ferromagnetic resonance to be α = 0.022, which is significantly lower than in Pt or Pd based magnetic multilayers. In zero magnetic field the critical current required to switch the free layer from the parallel to antiparallel alignment is 5.2 mA, and from antiparallel to parallel alignment is 4.9 mA. Given the volume of the free layer, V_{FL} = 1.01×10^{-22} m^3, the switching efficiency, $I_c/(V_{FL} \times \mu_0 H_c)$, is 5.28×10^{20} A/T·m^3, twice as efficient as any previously reported device with a similar structure.

Index Terms—**Magnetic and Spintronics Material, Spin transfer torque, magnetization reversal, Perpendicular Magnetic Anisotropy**

I. Introduction

SPIN transfer torque random access memory (STT-RAM) is one of the most promising emerging non-volatile memory technologies. It has a potential to be used as universal memory due to its high recording density, fast write/read speed (a few ns), unlimited endurance, excellent scalability and low power consumption [1]. Spin transfer torque is mostly studied in nanopillars that consist of two ferromagnetic layers separated by a thin non-magnetic layer. The first ferromagnetic layer, the reference layer (RL), is used to polarize the current which then passes through the non-magnetic (NM) layer without a significant change in polarization and interacts with the second ferromagnetic layer, the free layer (FL). This interaction leads to a transfer of angular momentum from the polarized current to the FL that is manifested as a torque on the FL. If the polarized current density is large enough, the spin torque will induce magnetization reversal in the FL [2], [3]. The device resistance depends on the relative orientation of the magnetic layers, the associated physical effect is giant magnetoresistance, GMR [4], [5], if NM is metallic, or tunnel magnetoresistance, TMR, if NM is an insulator [6]. In STT-RAM, information is recorded by inducing magnetization reversal in the FL. GMR or TMR is then used to detect the magnetization direction of the FL [7], [8].

The GMR effect is observed in two geometries, CIP (Current In Plane) and CPP (Current Perpendicular to Plane). In the CIP geometry, the current flows mainly in the NM layer due to its lower resistivity than that of the magnetic layers, which gives a non uniform current density. However, in the CPP geometry, the current flows in the whole layered structure and therefore the spin dependent scattering can be utilized more efficiently [9].

Corresponding author: M. Arora (email: mmonika@sfu.ca).

The TMR sensors are successfully applied to the read heads for the high density hard disk drives of areal density over 200 Gbit/in^2. For the devices with a TMR ratio of 50%, the RA product is of the order of 0.4 $\Omega(\mu m)^2$. The intrinsic sensor quantity RA is the product of the resistance R and the area A through which the current flows [10], [11]. To achieve higher areal density exceeding 500 Gbit/in^2, much lower RA product is required. A fully metallic CPP GMR devices with low RA product ($\approx$ 0.05 $\Omega(\mu m)^2$) may offer an alternative to the TMR sensors [9].

The main challenges for implementing STT writing mode in high density and high speed memory is the reduction of the critical current density, I_c, required to switch the magnetization of the FL while maintaining its thermal stability. In the macrospin approximation, the critical current required for spin-transfer reversal of the FL from the parallel (P) to anti-parallel (AP) and from the AP to P state is given by [12]

$$I_c \approx \left(\frac{2e}{\hbar}\right) \frac{\alpha M_s V_{FL}}{g(\theta)p} H_{eff} \quad (1)$$

where M_s, α, and V_{FL} are the saturation magnetization, Gilbert damping constant, and volume of the FL, respectively, p is the spin polarization of the current collinear with the RL magnetization, and $g(\theta)$ is an asymmetric pre-factor depending on the relative angle between RL and the FL [13], where θ can be either 0 for the P state or π for the AP state.

STT-RAM devices with both RL and FL with perpendicular magnetic anisotropy (PMA) are desired to lower I_c [14], [15]. The effective field acting on the perpendicularly magnetized FL [14], $H_{eff}^{P\rightarrow AP} = -H_{k\perp} + \mu_0 M_s + H_{app} + H_{dip}$ and $H_{eff}^{AP\rightarrow P} = H_{k\perp} - \mu_0 M_s + H_{app} + H_{dip}$, has contributions from the perpendicular uniaxial anisotropy field $H_{k\perp}$, demagnetizing field $\mu_0 M_s$, applied field H_{app}, and the dipolar field

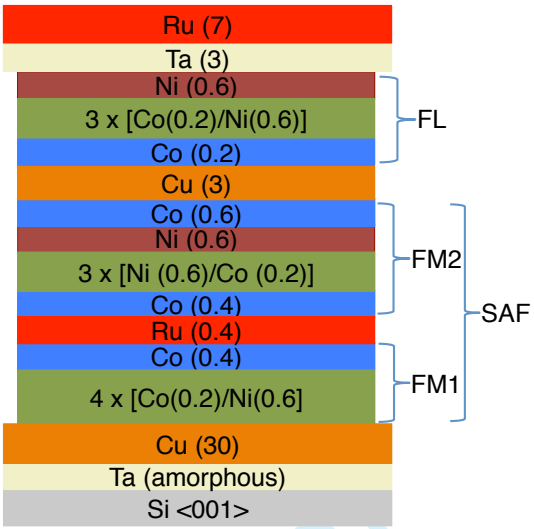

Fig. 1. Schematic representation of the film structure, Ta/Cu/SAF/Cu/FL/Ta.

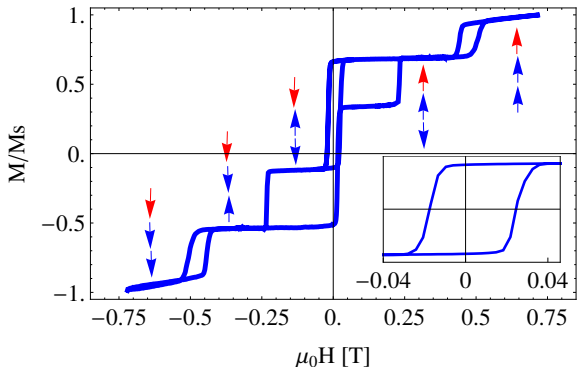

Fig. 2. Polar MOKE data of the Ta/Cu/SAF/Cu/FL/Ta structure, showing the reversal of individual layers with magnetic field. The hysteresis loop of the FL is also shown in the inset.

from the reference layer H_{dip}.

Following Equation 1 the optimum STT-RAM design would have magnetic layers with a high spin polarization and low damping. Also, $I_c^{P\to AP}$ has to be similar to $I_c^{AP\to P}$. This can be achieved by controlling the dipolar interaction between the RL and FL in order to compensate the asymmetry intrinsic to $g(\theta)$.

In most of the STT-RAM devices, both RL and FL are composed of a combination of Co/Pd, Co/Pt, Co/Ni and CoFe/Ni multilayers to obtain the large PMA [12], [16], [17]. The multilayers containing Pt or Pd (high Z elements) have high damping and low spin polarization, which decreases the spin torque efficiency of STT-RAM devices. Co/Ni multilayers are of particular interest to be used in our SAF layer design due to the low cost of Ni compared to Pt and Pd, tunable magnetization and PMA, low damping α and high spin polarization p [14], [18], [19].

The anisotropy and damping of Co(d_{Co})/Ni(d_{Ni}) multilayers depend on the thickness of Co, d_{Co}, and Ni, d_{Ni}, layers. The largest perpendicular magnetic anisotropy is obtained for d_{Co} = 0.2 nm and d_{Ni} = 0.6 nm, and it decreases with d_{Co} for $d_{Co} < 0.2$ nm and $d_{Co} > 0.2$ nm [20], [21]. The perpendicular magnetic anisotropy also decreases with d_{Ni} for $d_{Ni} > 0.6$ nm [22]. The damping decreases with increase of d_{Co}[18].

In this paper, we propose a design of nanopillars for STT-RAM devices consisting solely of Co/Ni multilayers. The extended films are highly optimized in order to maximize exchange coupling across the synthetic antiferromagnetic (SAF) layer and minimize the damping and dipolar field on the free layer. We are not aware of any investigations of devices with a SAF layer consisting only of Co/Ni multilayers. We choose Co/Ni multilayers with d_{Co} = 0.2 nm and d_{Ni} = 0.6 nm in order to maximize the PMA = 3.7 $\times 10^5$ J/m^3 ($\mu_0 H_k$ = -0.4 T), required for thermal stability of the FL.

II. Experimental Details

The magnetic multilayer films are deposited on Si(001) wafers by magnetron sputtering in a high vacuum deposition system with a base pressure of 5×10^{-8} Torr. The Si wafers are covered with a 100 nm SiO_2 layer to electrically isolate the wafer and metallic films. We deposited two film structures: 1) Ta(3)/Cu(30)/SAF/Cu/FL/Ta(3)/Ru(7) for fabrication of nanopillar devices (Figure 1), and 2) Ta(3)/Cu(10)/FL/Ta(3) for ferromagnetic resonance (FMR) measurements. The SAF consists of two FM layers, FM1 and FM2, antiferromagnetically coupled across a 0.4 nm thick Ru spacer layer. FM1 is composed of 4×[Co(0.2)/Ni(0.6)]/Co(0.4), FM2 is Co(0.4)/3×[Ni(0.6)/Co(0.2)]/Ni(0.6)/Co(0.6), and the FL is 4×[Co(0.2)/Ni(0.6)] (thicknesses are in nm). 3 nm of Cu is deposited as a spacer to decouple the SAF and the FL. The Ta/Cu bilayer structure helps set up the (111) growth orientation for Co/Ni multilayers. For corrosion protection, the films are covered by Ta/Ru and Ta.

The circular shaped nanopillars with SAF/Cu/FL film structure of diameter 200 nm were patterned by electron beam lithography and Ar^+ ion milling as described elsewhere [23]. Resistance of the nanopillar is measured in a 2-point geometry using standard microwave probes. The current direction was set so that for positive current, electrons flow from SAF to FL. The probe station was capable of applying over 1 T field both in-plane and normal to the film surface.

Magnetic measurements are performed on the continuous films before patterning. Kerr measurements of SAF/Cu/FL show that the magnetic coercivity, $\mu_0 H_c$, of the SAF and the FL in the continuous films is 0.23 T and 0.018 T, respectively as shown in the Figure 2. The hysteresis loop of the FL (inset in Figure 2) is shifted by less than 3 mT around zero field axis indicating weak interaction (the RKKY like and roughness induced magnetostatic couplings) between SAF and FL. The field dependence of the magnetization of the FL was measured using a superconducting quantum interference device (SQUID) magnetometer in magnetic fields up to 7 T. The measurements revealed a magnetization polarization of $\mu_0 M_s$ = 0.79 T. The magnetic properties of the FL were also measured with FMR with a co-planer waveguide in a field-swept, field-modulated configuration, as detailed by Montoya et al. [24]. The FMR measurements were performed in a frequency range between 15-32 GHz and with the DC field applied perpendicular to the film surface. The FMR linewidth is well described by Gilbert-

like damping.

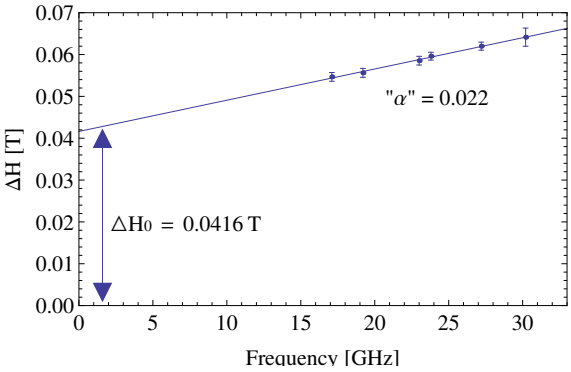

Fig. 3. FMR line width versus frequency measurements of the FL. The intrinsic damping α is calculated from the slope and ΔH_0 from the intercept.

$$\Delta H(f_0) = \Delta H_0 + \alpha \frac{2\pi f_0}{\gamma} \quad (2)$$

where f_0 is the microwave frequency and ΔH_0 is the zero frequency line broadening due to the long range homogeneity [25]. From the FMR measurements we found that the magnetic anisotropy constant of FL is K_u = 3.7×10^5 J/m^3 and g-factor is g = 2.193. The intrinsic Gilbert damping using Equation 2 is calculated to be α = 0.0221 and ΔH_0 = 0.0416 T as shown in Figure 3.

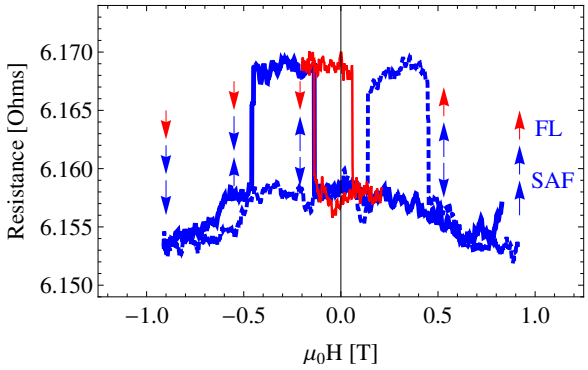

Fig. 4. Major and minor magnetoresistance loops for a 200 nm diameter pillar. Measurements performed with 0.5 mA DC current, and magnetic field applied perpendicular to the film surface. The arrows represent the directions of the magnetic moments of FM1 (bottom arrow), FM2 (middle arrow) and FL (top arrow) if the magnetic field is reduced from 0.8 to -0.8 T. Dashed line represents the change in resistance if the magnetic field is increased from -0.8 to 0.8 T. If the applied field is varied from -0.2 to 0.2 T the change in resistance is only due to the reversal of magnetization in the FL, red solid line.

III. Results and Discussion

The dc-resistance of a circular SAF/Cu/FL nanopillar of diameter 200 nm as a function of the applied field perpendicular to the surface of substrate is shown in Figure 4. In the measurements, the applied d.c. current is kept constant and equal to 0.5 mA. At positive saturation field, the direction of magnetic moments of all the FM layers in the structure are parallel to the direction of the applied field, corresponding to a state of lowest resistance. As the field is reduced, the magnetic moment of FM1 reverses first at 0.62 T due to the antiferromagnetic exchange coupling between FM1 and FM2. Since FM1 and FM2 have the similar film structure their magnetic anisotropy is similar. However, the Zeeman energy of FM1 is smaller than that of FM2 because the magnetization of FM1 is smaller than that of FM2. For this reason, the magnetic moment of FM1 in the SAF reverses first. The change from the P to AP alignment at 0.62 T between the magnetic moments of FM1 and FM2 in the SAF results in a slight increase in resistance.

Further reduction of the applied magnetic field causes the reversal of the magnetic moment in FL at $\mu_0 H = -0.13$ T. At this field, alignment between the magnetic moments of the adjacent magnetic layers are AP (FM1 and FM2 are AP, and FM2 and FL are AP) and hence resistance of the nanopillar increases to its highest value. The orientation of magnetic moments in the FM layers is unchanged from -0.13 T $< \mu_0 H < -0.49$ T. At $\mu_0 H$ = -0.49 T both magnetic layers in SAF (FM1 and FM2) simultaneously rotate. This sets the magnetic moment of the FL parallel to that of FM2 resulting in a decrease of the nanopillar resistance. Even at this field the antiferromagnetic coupling across Ru is strong enough to ensure that mutual alignment between magnetic moments of FM1 and FM2 stays AP. At negative saturation field, the magnetic moments of all the FM layers are aligned with the applied field, corresponding again to a state with the lowest resistance. The same trend is observed when the applied field sweeps from -0.8 to 0.8 T.

If the applied field is varied from -0.2 to 0.2 T (Figure 4 minor loop) the change of resistance is only due to the reversal of the FL; the SAF do not reverse. A comparatively higher field is required to reverse the magnetic moment of the FL from P to AP orientation than from the AP to P orientation with the magnetic moment of FM2. Both the dipole interaction between the SAF and FL, and 0.5 mA DC current used for GMR measurements help to stabilize the P state and therefore shift the hysteresis loop towards negative fields.

The change in resistance due to the transition from the P to AP alignment between the magnetic moments of FM1 and FM2 (Co/Ru/Co interface) is about two and a half times smaller than the change in resistance due to the transition from the P to AP alignment between the magnetic moments of FM2 and FL (Co/Cu/Co interface). The reduced GMR at the Co/Ru interface is due to the small difference between the spin-polarized density of states at the Fermi level [26] and also due to the possible inter-diffusion at Co/Ru interfaces [27]. The larger GMR from the Co/Cu/Co system is expected due to electronic structure at the Fermi level [13].

Compared to the extended film samples the nanopillar displays larger coercivities for both the SAF and the FL. The coercive field of the SAF reaches 0.49 T and that of the FL reaches 0.098 T. The increase of the coercivity field in both SAF and FL in nanopillars is due to size effects. In large magnetic structures, a defect or non-uniformity can act as a centre for a magnetic domain nucleation that causes the magnetization reversal at magnetic fields several orders of magnitude smaller than $2K_u/M_s$ (where K_u is the magnetic anisotropy energy and M_s is the saturation magnetization of

the magnetic structure). In nm-size magnetic structures much larger magnetic fields are required to nucleate a magnetic domain and cause the magnetization reversal [28] since the energy term due to the direct exchange interaction is dominant in nm-size structures.

The resistance as a function of d.c. current, measured at zero applied field, is shown in Figure 5. The critical current, I_c, required to reverse the magnetization of FL from P to AP alignment is I_c = 6.7 mA and from AP to P is I_c = 3.3 mA.

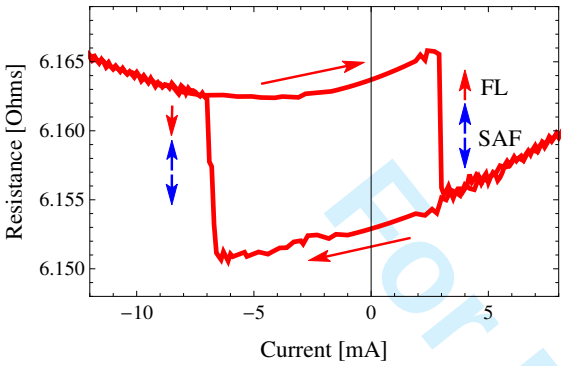

Fig. 5. Current induced switching of the FL between P and AP states at a zero applied magnetic field. The arrows represent the directions of the magnetizations of FM1 (bottom arrow), FM2 (middle arrow) and FL (top arrow).

Starting from either P or AP alignment of SAF and FL a series of the $R_{d.c.}$ versus H measurements are repeated for different values of applied current to construct a field-current phase diagram as shown in Figure 6. For each value of the applied current, the field sweeps from 0.2 T to -0.2 T. It is clear from the phase diagram that, at H_{app} + H_{dip} = 0 (H_{dip} = 22.5 mT), the current required to switch the FL from P to AP is around 5.2 mA (1.66×10^7A cm^{-2}) while to reverse the FL from AP to P is 4.9 mA (1.56×10^7A cm^{-2}). This is due to the spin-transfer-torque asymmetry in metallic spin-valve systems [2].

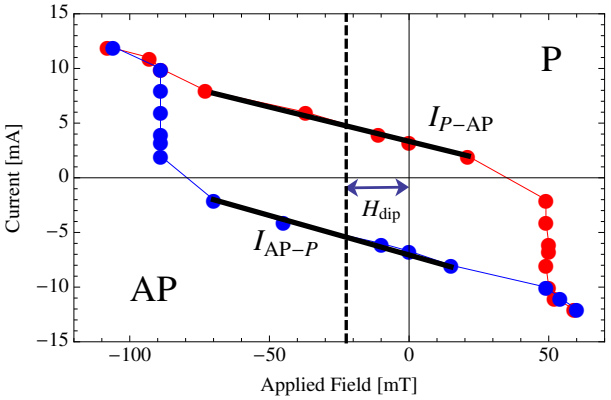

Fig. 6. Field-current phase diagram showing region where the FL is parallel and antiparallel to the SAF reference layer.

Figure 6 shows the linear dependance of I_c (P-AP) (with slope = -7.02 $\times$ 10^{-2} mA/mT) and I_c (AP-P) (with slope = -6.47 $\times$ 10^{-2} mA/mT) on the H_{app} for -70 mT $< H_{app} <$ 20 mT. This is in agreement with the Equation 1 and allows us to estimate the α/p ratio of the FL. This is done by substituting the slopes of I_c versus field to the pre-factor of Equation 1. The values of α/p calculated from our measurements are 0.33 $g(\pi)$ and 0.36 $g(0)$. These α/p values are similar to those obtained by Mangin et al. [14]. For $H_{app} <$ -90 mT and $H_{app} >$ 50 mT, I_c deviates from the linear behaviour of Equation 1, due in-parts to the finite temperature effects [29].

The efficiency of current induced magnetization reversal of the FL can be determined from the expression $I_c/(V_{FL}H_c)$, [12] where I_c is critical current, V_{FL} and H_c are the volume and coercivity of the FL, respectively. In our nanopillars V_{FL} = 1.01×10^{-22} m^3 and H_c = 0.098 T resulting in $I_c/(V_{FL}H_c)$ is 5.28×10^{20} A/T m^3. This is twice as efficient as what was reported previously for devices with SAF reference layer [12].

In that study, the FL comprised Co/Ni and Co/Pd multilayers. Co/Pd multilayers have higher damping than Co/Ni multilayers [30], [31]. We further reduced damping in our Co/Ni multilayers by increasing the Co to Ni thickness ratio (4×[Co(0.2)/Ni(0.6)]) as suggested by Shaw et al. [19] and Mizukami et al. [32]. We therefore attribute the lower damping to the increase in the efficiency (compared to Ref. [12]) of spin-torque driven switching in our nanopillars. It is also important to mention that the thermal fluctuations affect both I_c and H_c in a similar manner, therefore the coefficient describing the efficiency at temperature T is $I_c(T)/H_c(T) \approx I_{c0}/H_{c0}$, where I_{c0} and H_{c0} are the critical current and coercivity at zero temperature. Therefore, in a reasonable approximation, the ratio of I_c/H_c removes the temperature effects and remains close enough to its zero temperature value [33], [34].

IV. Conclusion

We investigate current and field induced magnetization reversal in perpendicularly magnetized 200 nm diameter circular nanopillars with a unique magnetic layer design: a Co/Ni multilayer free layer (FL), and a synthetic antiferromagnet (SAF) reference layer consisting of two antiferromagnetically coupled Co/Ni multilayers. In our nanopillars, the dipolar field acting on FL is only 22.5 mT, more than two times smaller than reported in devices with a single ferromagnetic reference layer [14]. Also, in our devices the current-induced magnetization reversal of FL is almost twice as efficient as reported for the devices with a SAF reference layer [12]. This is attributed to the low Gilbert damping of our FL corroborated by extended films ferromagnetic resonance studies.

Acknowledgment

Financial support for this project was provided by the Natural Sciences and Engineering Research Council of Canada (NSERC). Also, A.M.D., C.F., V.S. and E.K. acknowledge support from the Helmholtz Young Investigator Initiative Grant No. VH-N6-1048. Support from the Nanofabrication Facilities Rossendorf at the Ion Beam Centre is gratefully acknowledged.

References

[1] Y. Huai, "Spin-transfer torque MRAM (STT-MRAM): Challenges and prospects," *AAPPS Bulletin*, vol. 18, no. 6, pp. 33–40, 2008. [Online]. Available: http://wwhttp//www.cospa.ntu.edu.tw/aappsbulletin/data/18-6/33spin.pdf

[2] J. Slonczewski, "Current-driven excitation of magnetic multilayers," *Journal of Magnetism and Magnetic Materials*, vol. 159, no. 1-2, pp. L1–L7, Jun. 1996. [Online]. Available: http://linkinghub.elsevier.com/retrieve/pii/0304885396000625

[3] L. Berger, "Emission of spin waves by a magnetic multilayer traversed by a current," *Physical Review B*, vol. 54, no. 13, pp. 9353–9358, Oct. 1996. [Online]. Available: http://link.aps.org/doi/10.1103/PhysRevB.54.9353

[4] M. N. Baibich, J. M. Broto, A. Fert, F. N. Van Dau, and F. Petroff, "Giant Magnetoresistance of (001)Fe/(001)Cr Magnetic Superlattices," *Physical Review Letters*, vol. 61, no. 21, pp. 2472–2475, Nov. 1988. [Online]. Available: http://link.aps.org/doi/10.1103/PhysRevLett.61.2472

[5] G. Binasch, P. Grünberg, F. Saurenbach, and W. Zinn, "Enhanced magnetoresistance in layered magnetic structures with antiferromagnetic interlayer exchange," *Physical Review B*, vol. 39, no. 7, pp. 4828–4830, Mar. 1989. [Online]. Available: http://link.aps.org/doi/10.1103/PhysRevB.39.4828

[6] M. Julliere, "Tunneling between ferromagnetic films," *Physics Letters A*, vol. 54, no. 3, pp. 225–226, Sep. 1975. [Online]. Available: http://linkinghub.elsevier.com/retrieve/pii/0375960175901747

[7] M. Tsoi, A. G. M. Jansen, J. Bass, W. C. Chiang, M. Seck, V. Tsoi, and P. Wyder, "Excitation of a Magnetic Multilayer by an Electric Current," *Physical Review Letters*, vol. 80, no. 19, pp. 4281–4284, May 1998. [Online]. Available: http://link.aps.org/doi/10.1103/PhysRevLett.80.4281

[8] J. E. Wegrowe, D. Kelly, Y. Jaccard, P. Guittienne, and J. P. Ansermet, "Current-induced magnetization reversal in magnetic nanowires," *Europhysics Letters (EPL)*, vol. 45, no. 5, pp. 626–632, Mar. 1999. [Online]. Available: http://stacks.iop.org/0295-5075/45/i=5/a=626?key=crossref.0d8524430b85005e29e28f229fc52e2e

[9] J. Katine and E. E. Fullerton, "Device implications of spin-transfer torques," *Journal of Magnetism and Magnetic Materials*, vol. 320, no. 7, pp. 1217–1226, Apr. 2008. [Online]. Available: http://linkinghub.elsevier.com/retrieve/pii/S0304885307010189

[10] J. Bass, "CPP magnetoresistance of magnetic multilayers: A critical review," *Journal of Magnetism and Magnetic Materials*, vol. 408, pp. 244–320, Jun. 2016. [Online]. Available: http://linkinghub.elsevier.com/retrieve/pii/S0304885315308660

[11] I. Z. Evgeny Y. Tsymbal, *Handbook of Spin Transport and Magnetism*. CRC Press Book, 2011.

[12] I. Tudosa, J. A. Katine, S. Mangin, and E. E. Fullerton, "Perpendicular spin-torque switching with a synthetic antiferromagnetic reference layer," *Applied Physics Letters*, vol. 96, no. 21, p. 212504, 2010. [Online]. Available: http://scitation.aip.org/content/aip/journal/apl/96/21/10.1063/1.3441402

[13] J. Slonczewski, "Currents and torques in metallic magnetic multilayers," *Journal of Magnetism and Magnetic Materials*, vol. 247, no. 3, pp. 324–338, Jun. 2002. [Online]. Available: http://linkinghub.elsevier.com/retrieve/pii/S0304885302002913

[14] S. Mangin, D. Ravelosona, J. a. Katine, M. J. Carey, B. D. Terris, and E. E. Fullerton, "Current-induced magnetization reversal in nanopillars with perpendicular anisotropy," *Nature Materials*, vol. 5, no. 3, pp. 210–215, Feb. 2006. [Online]. Available: http://www.nature.com/doifinder/10.1038/nmat1595

[15] S. Le Gall, J. Cucchiara, M. Gottwald, C. Berthelot, C.-H. Lambert, Y. Henry, D. Bedau, D. B. Gopman, H. Liu, a. D. Kent, J. Z. Sun, W. Lin, D. Ravelosona, J. a. Katine, E. E. Fullerton, and S. Mangin, "State diagram of nanopillar spin valves with perpendicular magnetic anisotropy," *Physical Review B*, vol. 86, no. 1, p. 014419, Jul. 2012. [Online]. Available: http://link.aps.org/doi/10.1103/PhysRevB.86.014419

[16] Y. Jiang, G. H. Yu, Y. B. Wang, J. Teng, T. Ochiai, N. Tezuka, and K. Inomata, "Spin transfer in antisymmetric exchange-biased spin-valves," *Applied Physics Letters*, vol. 86, no. 19, p. 192515, 2005. [Online]. Available: http://scitation.aip.org/content/aip/journal/apl/86/19/10.1063/1.1927694

[17] D. B. Gopman, D. Bedau, S. Mangin, E. E. Fullerton, J. a. Katine, and a. D. Kent, "Bimodal switching field distributions in all-perpendicular spin-valve nanopillars," *Journal of Applied Physics*, vol. 115, no. 17, p. 17C707, May 2014. [Online]. Available: http://scitation.aip.org/content/aip/journal/jap/115/17/10.1063/1.4855019

[18] J.-M. Beaujour, W. Chen, K. Krycka, C.-C. Kao, J. Z. Sun, and a. D. Kent, "Ferromagnetic resonance study of sputtered Co—Ni multilayers," *The European Physical Journal B*, vol. 59, no. 4, pp. 475–483, Mar. 2007. [Online]. Available: http://www.springerlink.com/index/10.1140/epjb/e2007-00071-1

[19] J. M. Shaw, H. T. Nembach, and T. J. Silva, "Damping phenomena in Co90Fe10/Ni multilayers and alloys," *Applied Physics Letters*, vol. 99, no. 1, p. 012503, 2011. [Online]. Available: http://scitation.aip.org/content/aip/journal/apl/99/1/10.1063/1.3607278

[20] S. Girod, M. Gottwald, S. Andrieu, S. Mangin, J. McCord, E. E. Fullerton, J.-M. L. Beaujour, B. J. Krishnatreya, and A. D. Kent, "Strong perpendicular magnetic anisotropy in Ni/Co(111) single crystal superlattices," *Applied Physics Letters*, vol. 94, no. 26, p. 262504, 2009. [Online]. Available: http://scitation.aip.org/content/aip/journal/apl/94/26/10.1063/1.3160541

[21] M. Gottwald, S. Girod, S. Andrieu, and S. Mangin, "Tuneable perpendicular magnetic anisotropy in single crystal [Co/Ni](111) superlattices," *IOP Conference Series: Materials Science and Engineering*, vol. 12, p. 012018, Jun. 2010. [Online]. Available: http://stacks.iop.org/1757-899X/12/i=1/a=012018?key=crossref.7dee670043fe93b647575af4d2db3f85

[22] F. den Broeder, E. Janssen, W. Hoving, and W. Zeper, "Perpendicular magnetic anisotropy and coercivity of Co/Ni multilayers," *IEEE Transactions on Magnetics*, vol. 28, no. 5, pp. 2760–2765, 1992. [Online]. Available: http://ieeexplore.ieee.org/lpdocs/epic03/wrapper.htm?arnumber=179619

[23] M. Arora, C. Fowley, T. Mckinnon, E. Kowalska, V. Sluka, and A. M. Deac, "STT-RAM Memory Devices," *Physics in Canada*, vol. 72, no. 2, 2016.

[24] E. Montoya, T. McKinnon, A. Zamani, E. Girt, and B. Heinrich, "Broadband ferromagnetic resonance system and methods for ultrathin magnetic films," *Journal of Magnetism and Magnetic Materials*, vol. 356, pp. 12–20, Apr. 2014. [Online]. Available: http://linkinghub.elsevier.com/retrieve/pii/S0304885313009256

[25] B. Heinrich and J. Cochran, "Ultrathin metallic magnetic films: magnetic anisotropies and exchange interactions," *Advances in Physics*, vol. 42, no. 5, pp. 523–639, Oct. 1993. [Online]. Available: http://www.tandfonline.com/doi/abs/10.1080/00018739300101524

[26] T. Kai, Y. Ohashi, and K. Shiiki, "Study of giant magnetoresistance in Co/X superlattices (X= Cu, Ru, Rh and Pd) by first-principle band calculation," *Journal of magnetism and magnetic materials*, vol. 183, pp. 292–298, 1998. [Online]. Available: http://www.sciencedirect.com/science/article/pii/S0304885397010664

[27] S. Zoll, A. Dinia, J. P. Jay, C. Mény, G. Z. Pan, A. Michel, L. El Chahal, V. Pierron-Bohnes, P. Panissod and H. A. M. V. den Berg, "No Title," *Phys. Rev. B*, vol. 57, no. 8, p. 4842, 1998.

[28] E. Girt, K. Krishnan, and G. Thomas, "Optimization of magnetic properties of nanostructured Nd-Fe-B: approaching ideal Stoner-Wohlfarth behaviour," *Scripta Materialia*, vol. 44, no. 8-9, pp. 1431–1435, May 2001. [Online]. Available: http://linkinghub.elsevier.com/retrieve/pii/S1359646201009368

[29] D. Lacour, J. a. Katine, N. Smith, M. J. Carey, and J. R. Childress, "Thermal effects on the magnetic-field dependence of spin-transfer-induced magnetization reversal," *Applied Physics Letters*, vol. 85, no. 20, p. 4681, 2004. [Online]. Available: http://scitation.aip.org/content/aip/journal/apl/85/20/10.1063/1.1819516

[30] J. M. Shaw, H. T. Nembach, and T. J. Silva, "Determination of spin pumping as a source of linewidth in sputtered Co 90 Fe 10 /Pd multilayers by use of broadband ferromagnetic resonance spectroscopy," *Physical Review B*, vol. 85, no. 5, p. 054412, Feb. 2012. [Online]. Available: http://link.aps.org/doi/10.1103/PhysRevB.85.054412

[31] S. Pal, B. Rana, O. Hellwig, T. Thomson, and A. Barman, "Tunable magnonic frequency and damping in [Co/Pd][sub 8] multilayers with variable Co layer thickness," *Applied Physics Letters*, vol. 98, no. 8, p. 082501, 2011. [Online]. Available: http://scitation.aip.org/content/aip/journal/apl/98/8/10.1063/1.3559222

[32] S. Mizukami, X. Zhang, T. Kubota, H. Naganuma, M. Oogane, Y. Ando, and T. Miyazaki, "Gilbert Damping in Ni/Co Multilayer Films Exhibiting Large Perpendicular Anisotropy," *Applied Physics Express*, vol. 4, no. 1, p. 013005, Jan. 2011. [Online]. Available: http://stacks.iop.org/1882-0786/4/013005

[33] S. Mangin, Y. Henry, D. Ravelosona, J. a. Katine, and E. E. Fullerton, "Reducing the critical current for spin-transfer switching of perpendicularly magnetized nanomagnets," *Applied Physics Letters*, vol. 94, no. 1, p. 012502, 2009. [Online]. Available: http://scitation.aip.org/content/aip/journal/apl/94/1/10.1063/1.3058680

[34] M. P. Sharrock, "Time dependence of switching fields in magnetic recording media (invited)," *Journal of Applied Physics*, vol. 76, no. 10, pp. 6413–6418, Nov. 1994. [Online]. Available: http://scitation.aip.org/content/aip/journal/jap/76/10/10.1063/1.358282